Supplementary Material: The inviscid incompressible limit of Kelvin–Helmholtz instability for plasmas

Contents of the document: Figures S1, S2, S3, S4 and Table S1 in five sections.

This Supplementary Material contains additional results regarding the variations of some parameters, such as the Atwood number and the mean magnetic field intensity. The main outcomes, which are not essential for the global understanding of the study, are reported in the main text.

1. Spatial resolution in GAMERA for $\mathcal{A} = 0.05$

As a complement of the effects of varying the Mach number in figure 2a, we briefly address here the question of spatial resolution in GAMERA for the hydrodynamic simulations with Mach number $M = 0.134$ and the SM initial condition. In figure S1, there is an overall good agreement between the resolutions with 512^2, 1024^2 and 2048^2 points. When considering the density variance $\langle \rho'^2 \rangle$, we find that 1024^2 at least is required for convergence. A resolution of 2048^2 is thus chosen for the whole study.

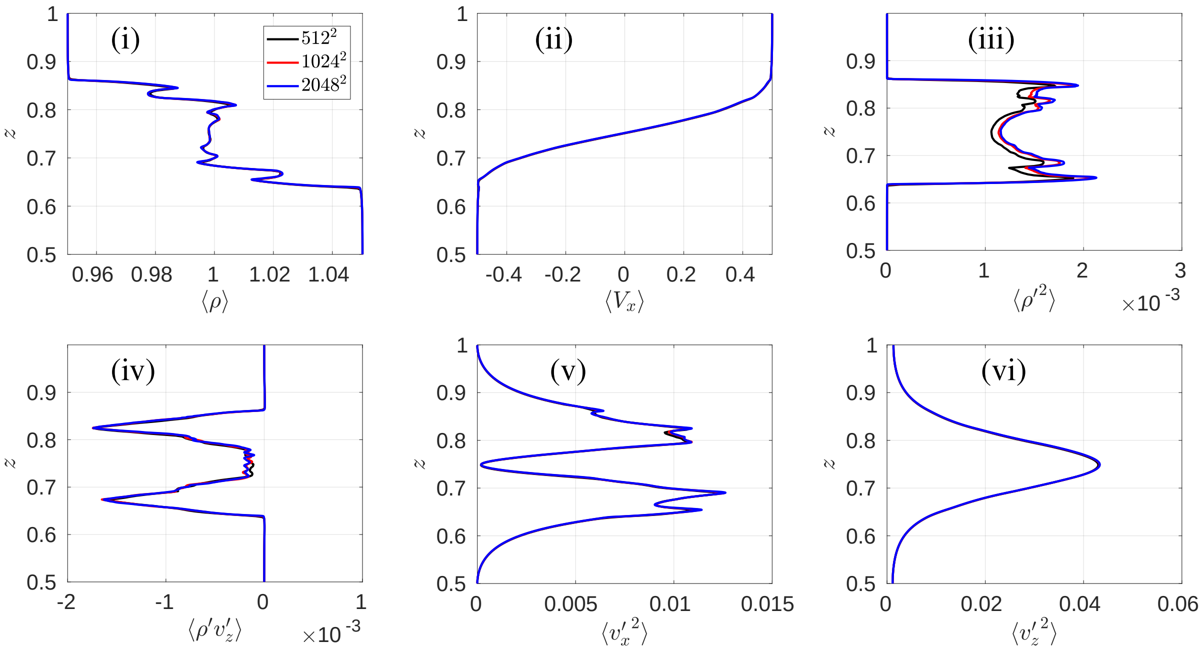

Figure S1: Hydro simulations for GAM ($M = 0.134$) with $\mathcal{A} = 0.05$ at $t = 3.0$. Effect of resolution on (i) Mean density $\langle \rho \rangle$, (ii) Mean horizontal velocity $\langle V_x \rangle$, (iii) Density variance $\langle \rho'^2 \rangle$, (iv) Vertical mass flux $\langle v_z' \rho' \rangle$, (v) Horizontal kinetic energy $\langle {v_x'}^2 \rangle$, (vi) Vertical kinetic energy $\langle {v_z'}^2 \rangle$.

2. Smaller density contrasts with $\mathcal{A} = 0.01$

We evaluate if the asymmetry observed in the GAMERA simulations decreases as $\mathcal{A}$ decreases. To this aim, one must verify that the Mach number $M = 0.134$ remains sufficiently small to reach the incompressible

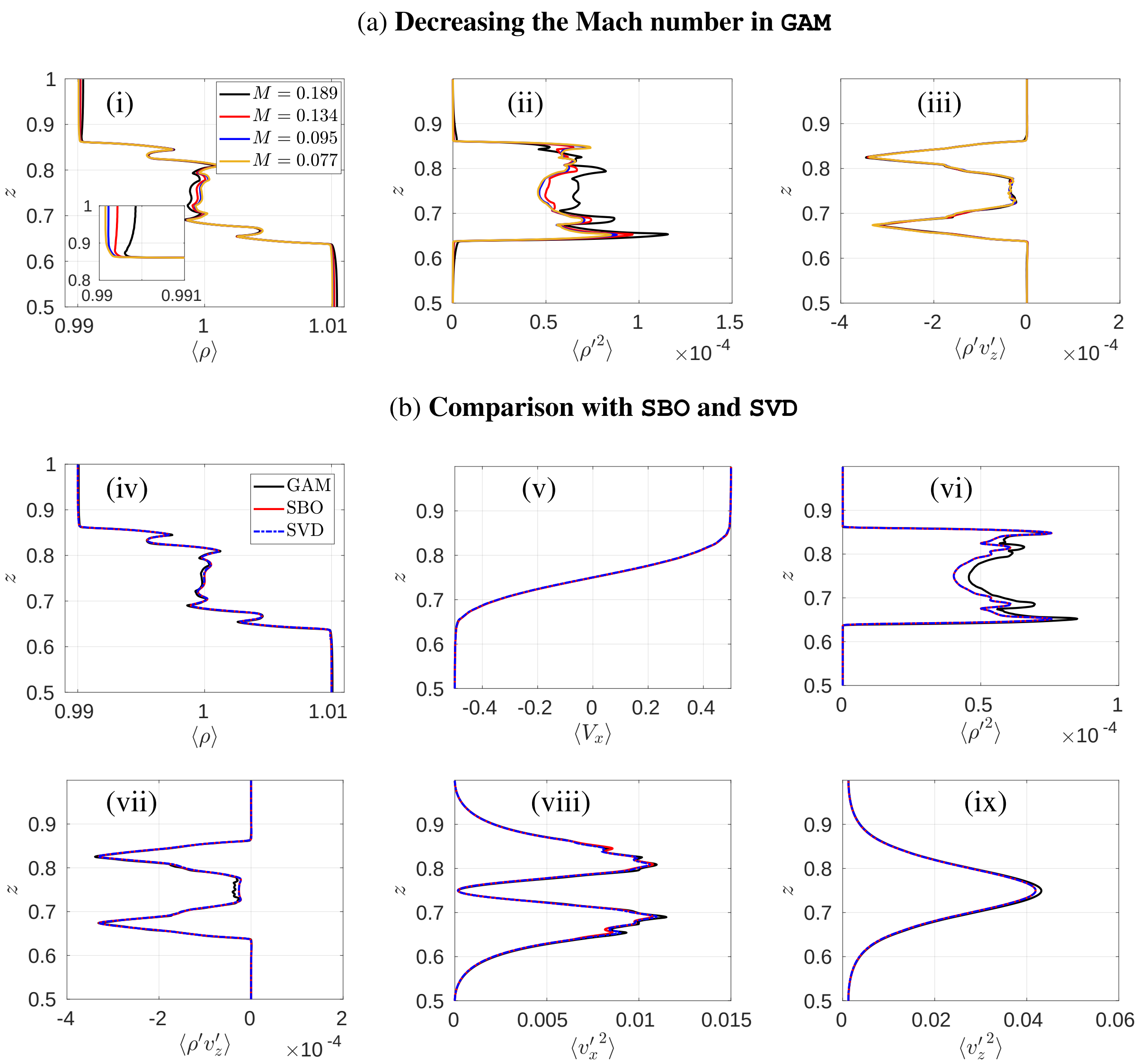

Figure S2: Hydro simulations (1024^2) for `GAM` with $\mathcal{A} = 0.01$ at $t = 3.0$. (a) Effect of Mach number M. (b) Comparison with `SBO` and `SVD`. (i) Mean density $\langle\rho\rangle$, (ii) Density variance $\langle\rho'^2\rangle$, (iii) Vertical mass flux $\langle v'_z\rho'\rangle$, (iv) Mean density $\langle\rho\rangle$, (v) Mean velocity $\langle V_x\rangle$, (vi) Density variance $\langle\rho'^2\rangle$, (vii) Vertical mass flux $\langle v'_z\rho'\rangle$, (viii) Horizontal kinetic energy $\langle {v'_x}^2\rangle$, (ix) Vertical kinetic energy $\langle {v'_z}^2\rangle$.

limit for such a small density contrast. Hence, the reference pressure P_0 controlling the Mach number is varied in `GAMERA` for $\mathcal{A} = 0.01$ and 1024^2 points with a SM perturbation in figure S2a.

We find that $M = 0.134$ (corresponding to $P_0 = 40$) was small enough for $\mathcal{A} = 0.05$, but not anymore for $\mathcal{A} = 0.01$. Looking at the density variance $\langle\rho'^2\rangle$, we see that decreasing the Mach number tends to restore symmetry (decreasing the bottom peak and increasing the top one).

In the inset of figure S2a, we show that the error on the upper pure fluid density is of order 2 to 3% of $\mathcal{A}$ for $M = 0.134$, and reduces as the Mach number decreases to $M = 0.095$ and $M = 0.077$. We find that $M = 0.077$ is required for `GAMERA` at $\mathcal{A} = 0.01$, which we retain for the results presented in figure S2b.

There are two outcomes. First, the agreement is now much better between the SBO and SVD simulations, compared with the $\mathcal{A} = 0.05$ case in figure 4a, either for the mean fields $\langle\rho\rangle$ and $\langle V_x\rangle$, or for $\langle {v'_x}^2\rangle$. Second, the agreement with GAMERA is also very satisfactory thanks to the decrease in Mach number, though still not perfect. The differences in intensity for the density variance $\langle {\rho'}^2\rangle$ remain attributed to viscosity and diffusion in the STRATOSPEC simulations.

3. Larger density contrasts with $\mathcal{A} = 0.33$

For completeness, we address here the large density contrast case developed in McNally et al. (2012) with $\mathcal{A} = 1/3$. For such a density contrast, outside the Boussinesq limit, the codes GAMERA and STRATOSPEC must be compared in the Variable-Density framework: hence, the Mach number needs to be decreased once again in GAMERA to reduce compressibility effects. We settle for $M = 0.134$, value which was chosen for $\mathcal{A} = 0.05$ in section 3. For STRATOSPEC, the Variable-Density version is used (SVD).

The instantaneous density field is first shown in figure S3a for both GAM and SVD in the SM case. The agreement between the two codes is excellent for $t = 1$ and $t = 2$, with the displacement of the vortices well captured. At $t = 3$, unlike figure 3 for $\mathcal{A} = 0.05$, there are strong secondary small-scale shear instabilities in GAM, which is reminiscent of McNally et al. (2012) and due to baroclinic torque (Reinaud et al., 2000). These perturbations are absent in the SVD simulation because they are smoothed out by non-zero scalar diffusion.

Horizontally averaged profiles follow in figure S3b. The overall trend is captured, unlike the oscillations, as expected. The "bump" or overshoot in the mean horizontal velocity profile at $z \simeq 0.68$, where it becomes more intense than the imposed initial field ($|\langle V_x\rangle| \geq 0.5$), is well captured by both codes. The absence of small-scale instabilities in SVD causes significant differences with GAM when comparing second-order correlations such as $\langle v'_z\rho'\rangle$ and $\langle {v'_x}^2\rangle$. Moreover, the advection of the vortices is also well captured. The displacement is more pronounced here than for $\mathcal{A} = 0.05$ in figure 3 because the advection is stronger for larger density contrasts (Dimotakis, 1986).

Finally, for informative purposes, the case $M = 0.535$ is shown as well for GAM. It is clear that decreasing the Mach number down to $M = 0.134$ is essential for reaching the Variable-Density limit and obtain a quantitatively acceptable comparison.

4. Smaller mean magnetic field with $B_0 = 0.1$

We perform an additional comparison between STRATOSPEC and GAMERA for the SM perturbation with a mean magnetic field intensity $B_0 = 0.1$ lower than $B_0 = 0.2$ in section 4. In this case, vortices are much more distorted and survive until $t = 3$, as shown in figure 7a. The comparison of horizontally averaged profiles is shown in figure S4, where we see that the agreement between the simulations of both codes is again quite satisfactory.

5. Polynomial interpolation functions associated with the growth rate stability curves

Table S1 contains the coefficients associated with the polynomial interpolation functions curves in figure 14.

(a) **Density fields**

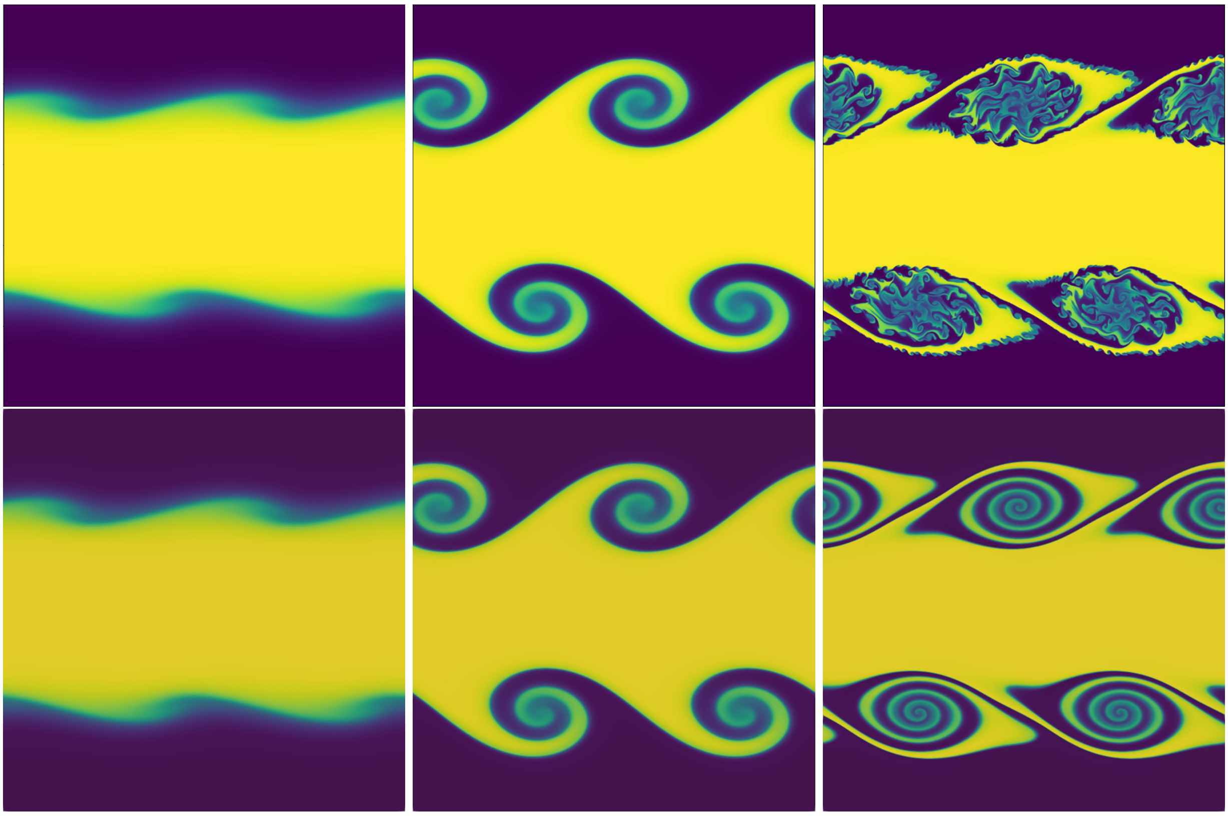

(b) **Horizontally averaged profiles**

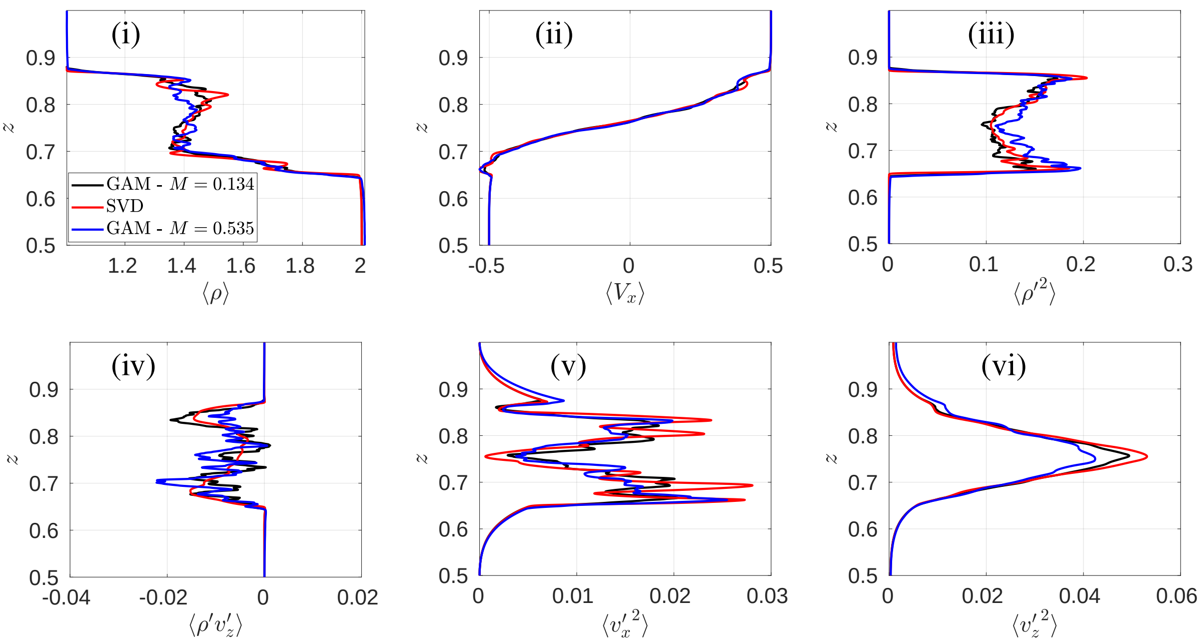

Figure S3: Hydro simulations (2048^2) for GAM ($M = 0.134$) and SVD with $\mathcal{A} = 0.33$. (a) Density field for GAM (top) and SVD (bottom) at $t = 1.0$, $t = 2.0$ and $t = 3.0$. (b) Horizontally averaged profiles for (i) Mean density $\langle \rho \rangle$, (ii) Mean velocity $\langle V_x \rangle$, (iii) Density variance $\langle \rho'^2 \rangle$, (iv) Vertical mass flux $\langle v_z' \rho' \rangle$, (v) Horizontal kinetic energy $\langle {v_x'}^2 \rangle$, (vi) Vertical kinetic energy $\langle {v_z'}^2 \rangle$.

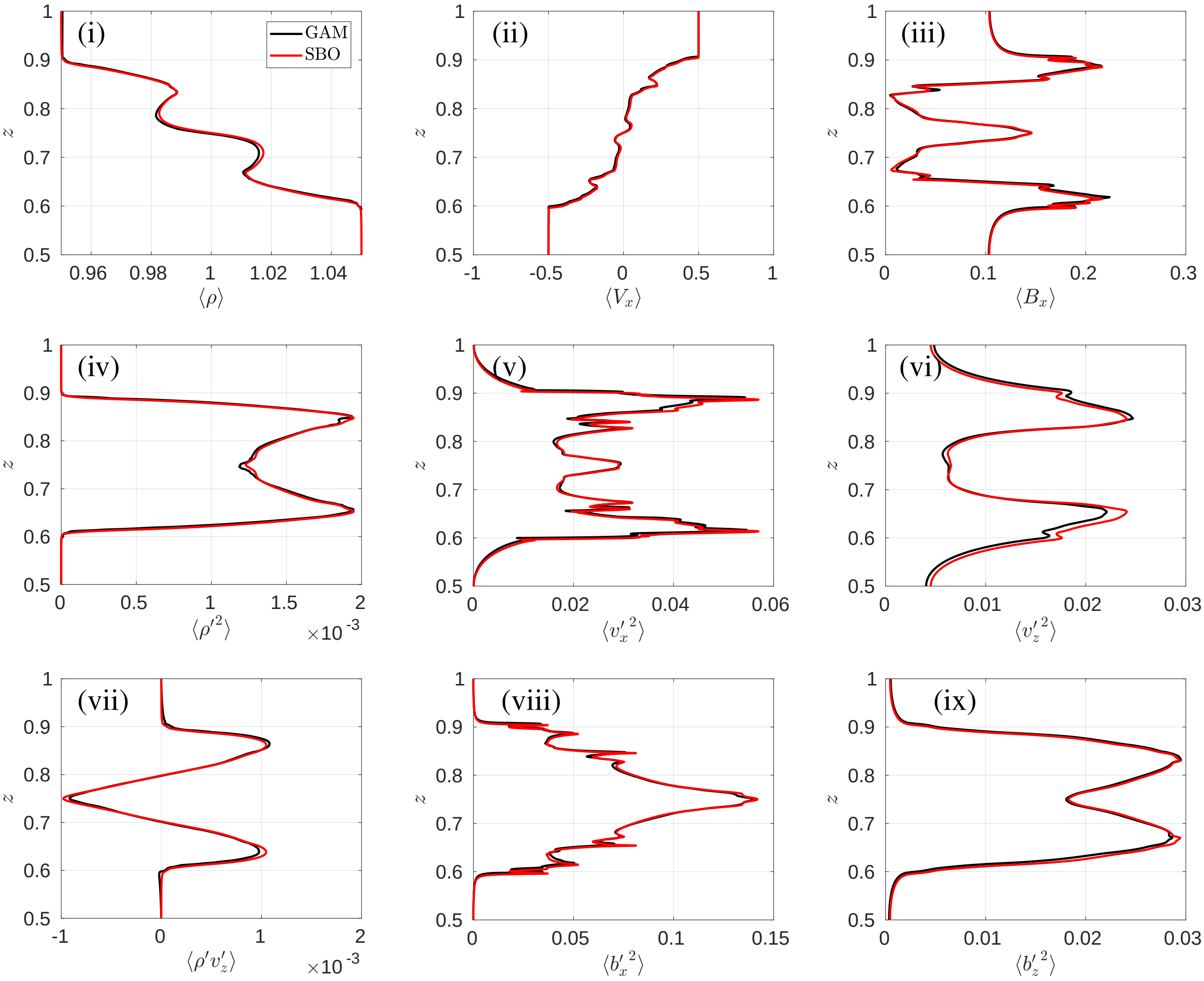

Figure S4: MHD simulations (2048^2) with $\mathcal{A} = 0.05$ and $B_0 = 0.1$ at $t = 3.0$, for GAM and SBO. (i) Mean density $\langle\rho\rangle$, (ii) Mean horizontal velocity $\langle V_x\rangle$, (iii) Mean horizontal magnetic field $\langle B_x\rangle$ (iv) Density variance $\langle\rho'^2\rangle$, (v) Horizontal kinetic energy $\langle {v_x'}^2\rangle$, (vi) Vertical kinetic energy $\langle {v_z'}^2\rangle$, (vii) Vertical mass flux $\langle v_z'\rho'\rangle$, (viii) Horizontal magnetic energy $\langle {b_x'}^2\rangle$, (ix) Vertical magnetic energy $\langle {b_z'}^2\rangle$.

Polynomial interpolation function $P(x) = a_4x^4 + a_3x^3 + a_2x^2 + a_1x + a_0$				
	$M = 0.535$			
	$B_0^{-1} = 0$	$B_0^{-1} = 0.2$	$B_0^{-1} = 0.3$	$B_0^{-1} = 0.4$
a_0	0	0	0	0
a_1	0.488	0.466	0.409	0.228
a_2	-0.0227	-0.0261	-0.0263	-0.0119
a_3	4.35×10^{-4}	6.50×10^{-4}	6.93×10^{-4}	0
a_4	-4.68×10^{-6}	-8.47×10^{-6}	-9.30×10^{-6}	0
	$M = 0.134$			
	$B_0^{-1} = 0$	$B_0^{-1} = 0.2$	$B_0^{-1} = 0.3$	$B_0^{-1} = 0.4$
a_0	0	0	0	0
a_1	0.505	0.474	0.412	0.227
a_2	-0.0223	-0.0247	-0.0245	-0.0128
a_3	3.96×10^{-4}	5.54×10^{-4}	5.23×10^{-4}	0
a_4	-4.01×10^{-6}	-6.40×10^{-6}	-5.67×10^{-6}	0

Table S1. Coefficients associated with the polynomial interpolation functions that fit the $(2k_xa,\ 2\gamma a/V_0)$ curves in figure 14, obtained with the `GAMERA` code for different magnetic fields B_0 and sonic Mach numbers M.